IEEE Access
Multidisciplinary | Rapid Review | Open Access Journal

Received July 10, 2019, accepted July 21, 2019, date of publication July 29, 2019, date of current version August 12, 2019.

Digital Object Identifier 10.1109/ACCESS.2019.2931772

Antenna Gain Enhancement by Using Low-Infill 3D-Printed Dielectric Lens Antennas

BILAL TARIQ MALIK, (Student Member, IEEE), VIKTOR DOYCHINOV, SYED ALI RAZA ZAIDI, (Member, IEEE), IAN D. ROBERTSON, (Fellow, IEEE), AND NUTAPONG SOMJIT, (Senior Member, IEEE)

School of Electronic and Electrical Engineering, University of Leeds, Leeds LS2 9JT, U.K.

Corresponding author: Bilal Tariq Malik (elbtm@leeds.ac.uk)

This work was supported by the Engineering and Physical Sciences Research Council, U.K., under Grant EP/N010523/1.

ABSTRACT This paper reports on the design and three-dimensional (3D) integration of low-cost, low-loss and easy-to-fabricate 3D-printed integrated lens antennas (ILAs) for 5G broadband wireless communications in the 28 GHz frequency range. The ILA designs consist of an extended hemispherical lens, fed by two different types of source antennas, a substrate integrated waveguide (SIW) slot antenna array and a microstrip patch antenna (MPA) array. Results from comprehensive parametric analyses of the infill pattern and density of the 3D printed dielectric lenses are also intensively investigated and characterized for their electromagnetic properties, e.g., electric-field distribution. The ILAs are fabricated using polylactic acid (PLA) as the fused deposition modelling (FDM) polymer with an optimized infill density of 50%, which speeds up prototyping time and decreases the relative permittivity, dielectric loss, manufacturing cost, and overall mass of the lens. These features are illustrated through experimental verification and characterization of at least three samples. From the measurement results, the ILAs achieve a fractional bandwidth of 10.7%, ranging from 26.5 to 29.4 GHz with a maximum gain of 15.6 dBi at boresight and half power beam-width of approximately 58° and 75° in the E and H planes, respectively.

INDEX TERMS 5G, integrated lens antennas, 3D printed, millimeter-wave antennas, microstrip patch antennas (MPA), substrate integrated waveguide (SIW).

I. INTRODUCTION

Future fifth-generation (5G) wireless communication systems are expected to enhance reliability and drastically increase data rates to an ever-growing number of mobile users and Internet-of-Things (IoT) devices [1]. To address this increase in telecommunication traffic requirements, portions of the underused millimeter-wave spectrum have been offered by regulators and used by service operators worldwide for fixed wireless access [2]. Candidate bands include 28 GHz, 38 GHz, 39 GHz, as well as 26 GHz, recently recommended by the United Kingdom's regulatory body, Ofcom [2].

However, millimeter-wave communication systems have limited range due to higher path loss and atmospheric attenuation and absorption [2]. This drawback has motivated the research to develop efficient and high-gain antennas, especially in the Ka band for 5G mobile communication. Currently, several solutions have been proposed to address this issue of limited range due to higher path loss at millimeter-wave frequencies [3], [4]. A particularly attractive and cost-effective method is gain enhancement using dielectric lenses, placed on top of source antennas such as microstrip patch antennas (MPAs) or substrate integrated waveguide (SIW) slot antennas [5]–[7]. These are also known as integrated lens antennas (ILAs). The dielectric lens increases the directivity of the source antenna by transforming the spherical wave front of the radiated wave into a planar one [5], [8]. MPAs and SIW slot antennas are preferable for source antennas, due to the ease of their fabrication, straightforward integration with other planar circuits, low mass, and low profile [9]–[11].

3D printed lens antennas are already extensively used in the upper millimeter-wave frequency region, as evidenced by recent research, reported in [12]–[14]. A waveguide fed 3D printed lens antenna for the 60 GHz millimeter-wave Industrial, Scientific and Medical (ISM) band is presented in [4]. Industrial poly-jet 3D printing was used to manufacture the hemispherical lens, which provided gain enhancement

The associate editor coordinating the review of this manuscript and approving it for publication was Mohammad Tariqul Islam.

This work is licensed under a Creative Commons Attribution 4.0 License. For more information, see http://creativecommons.org/licenses/by/4.0/

of the source antenna. Another 3D printed ''meta-lens'' is proposed in [7] for gain enhancement at Ka band. The lens provided gain improvement of 7.5 dB at 32.5 GHz.

Recently, a combination of 3D printed dielectric lens and dielectric polarizers have also been reported for polarization conversion, in addition to gain enhancement at millimeter-wave frequencies [15], [16]. The drawbacks of these polarizers are fabrication complexity, lower gain enhancement, and more losses when compared to a stand-alone dielectric lens. The polarizers also increase the overall footprint of the antenna.

Most of the dielectric lens antennas reported in the literature have high manufacturing cost and excessive weight due to the use of expensive and dense dielectric materials such as quartz, in addition to costly fabrication techniques [17], [18]. Furthermore, gain improvement due to the addition of these lenses is not always quantified and reported in these works.

The use of commercially-available 3D printers for the quick and cost-effective prototyping of dielectric lens antennas has recently increased rapidly [8]. However, most reported results use industry-grade printers such as Stratasys ^{TM}or slower and more expensive fabrication techniques such as stereolithography (SLA) [8], [17]. Dielectric lenses fabricated through desktop 3D printers using fused deposition modelling (FDM) technology tend to be printed as solid objects (100% infill density), which increases the cost and weight of ILAs and decreases the radiation efficiency due to the high dielectric losses of FDM materials [6], [19]–[21].

In this work, the design and implementation of low-cost, low-loss, easy to fabricate and integrate dielectric lens antennas at 28 GHz are reported. The fabrication process features commercially available desktop 3D printer, CEL Robox RBX02-DM, using standard FDM process. The ILAs were fabricated with a reduced infill percentage of 50%, which speeds up prototyping time, and simultaneously decreases dielectric loss, manufacturing cost and weight. At the same time, the lens antennas provide considerable gain enhancement of 6 dB, for two different types of source antennas - a 2x1 MPA array and a SIW slot antenna array. These were jointly designed and optimized to operate over the cluster of 5G candidate bands around 28 GHz. A parametric analysis on infill density and infill pattern of dielectric lenses and free space dielectric characterization of Polylactic Acid (PLA) with reduced infill densities have also been experimentally verified and are presented.

II. DIELECTRIC CHARACTERIZATION OF PLA HAVING DIFFERENT INFILL DENSITIES

To accurately design and simulate the 3D printed dielectric lens antennas with reduced infill density, the effect on the complex relative permittivity of the 3D printed samples needs to be quantified. For this purpose, three PLA samples with dimensions of 50 x 50 x 25 mm^3 were fabricated using 25%, 50%, and 75% infill density. The resulting fabrication parameters of these samples are summarized in Table 1.

TABLE 1. Effect of infill density on the fabrication parameters.

Metric	25 % Infill	50 % Infill	75 % Infill
Dielectric constant at 28 GHz	1.45	1.78	2.1
Loss tangent at 28 GHz	0.01	0.025	0.04
3D Printing time (HH/MM)	01:05	01:41	02:11
PLA Sample Mass (gram)	30.1	45	60.2
PLA Sample Cost (£)	0.79	1.6	2.39

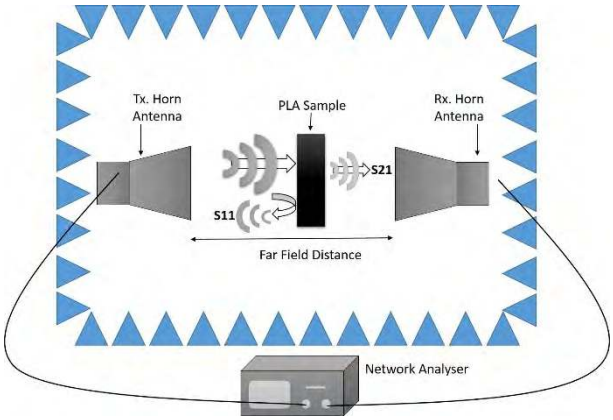

FIGURE 1. Free space measurement setup for dielectric characterization of PLA samples having different infill densities.

The Keysight Technologies^{TM}85071 free-space measurement software was used to measure the dielectric properties of the PLA samples having different infill densities over the frequency range of 26 - 32 GHz. Fig. 1 shows the measurement setup for the complex relative permittivity, with results from the free-space measurements given in Fig. 2(a) and Fig. 2(b). Two standard gain Ka-band horn antennas were used for transmission and reception of signals through PLA samples for dielectric measurements. Each sample was measured 3-4 times from different sides and using different distances, i.e. 25-40 cm, between the antennas to minimize the measurement error due to the anisotropic nature of PLA samples.

Measured results show that the relative permittivity and dielectric loss linearly decrease with a reduction in the infill density of PLA samples from 100% to 25%. The values of dielectric constant and loss tangent for different infill densities at 28 GHz are given in Table 1. Reduction of infill density also shows a clear impact on the fabrication time, weight and production cost, as summarized in Table 1.

III. IMPACT OF INFILL PATTERN AND INFILL DENSITY ON 3D PRINTED DIELECTRIC LENS

An extensive set of simulations, using Ansys HFSS^{TM}, was carried out to analyze the effects of infill pattern and infill density on the radiation properties of the 3D printed dielectric lenses. Three different types of infill pattern (rectilinear, triangle and honeycomb) with different infill densities (25%, 50% and 75%) were studied in the analyses. Figs. 3(a), 3(b), and 3(c) show the surface current distributions at the top of

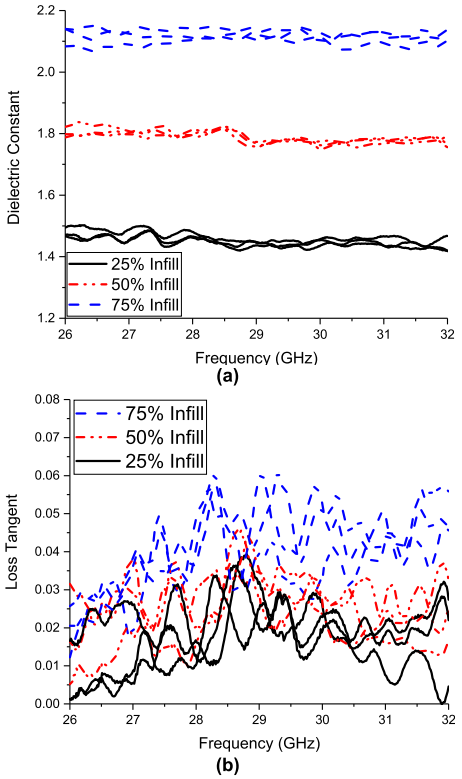

FIGURE 2. (a). Dielectric constant and (b). Loss tangent of PLA samples having different infill densities from 26 GHz to 32 GHz, measured using the Keysight Technologies 85071E material characterization suite.

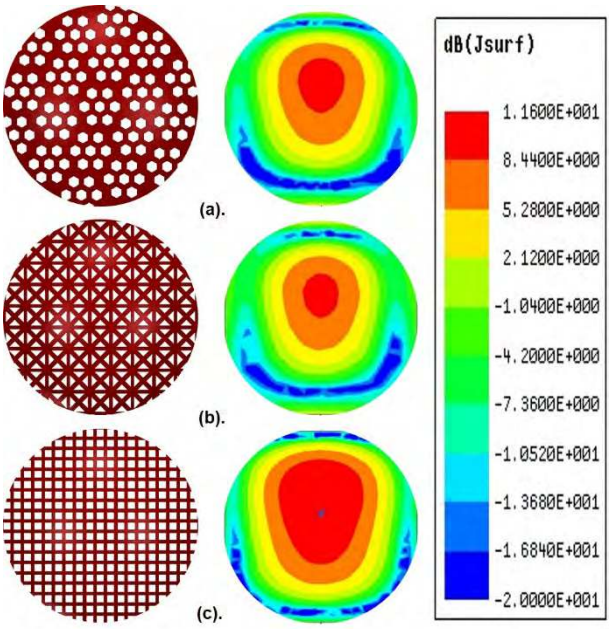

FIGURE 3. Infill patterns with surface current distribution on top of 3D printed dielectric lens, (a). Honeycomb, (b). Triangle, (c). Rectilinea.

the dielectric lens at 28 GHz for the three different infill patterns, respectively. It is evident that the dielectric lens with a rectilinear infill pattern has the strongest surface current density due to less inhomogeneity in its structure as compared

TABLE 2. Effect of infill pattern on the antenna parameters.

Parameters	Infill Pattern		
	Rectilinear	Triangle	Honeycomb
Gain (dB)	12.1	11.6	12.4
Radiation Efficiency (%)	82	76	78
Side Lobe Levels (dB)	-30	-22	-22
Return Loss (dB)	58	30	45
Simulation/Fabrication Time	Minimum	Moderate	Maximum
Surface Current Density (A/m)	3.6	2.2	2.7
Design Complexity	Low	Medium	High

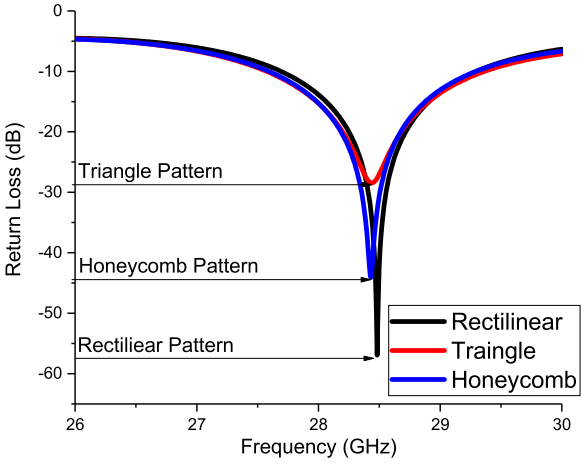

FIGURE 4. Impact of different infill pattern of dielectric lens on the reflection coefficien.

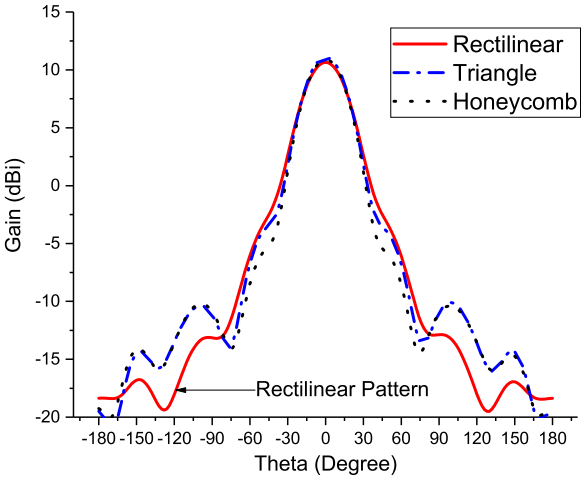

FIGURE 5. Impact of different Infill patterns of dielectric lens on Radiation Pattern.

to the other two patterns. Table 2 summarizes the simulated antenna parameters for the different infill patterns.

Fig. 4 and Fig. 5 depict the impact of the different infill patterns on the performance of the dielectric lenses in terms of reflection coefficient and radiation pattern, respectively. Rectilinear infill pattern shows the best impedance matching with return loss of less than 50 dB as compared to 30 dB and 45 dB for triangle and honeycomb infill patters, respectively.

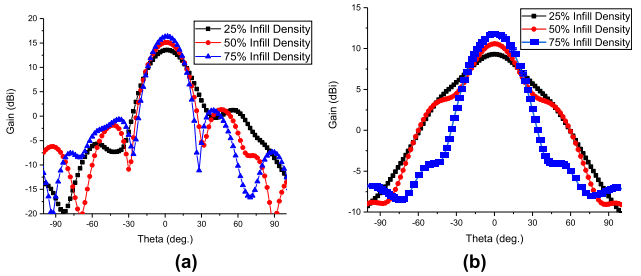

FIGURE 6. Radiation pattern of ILAs at 28 GHz for different infill densities of dielectric lens materials (a). SIW (b). MPA.

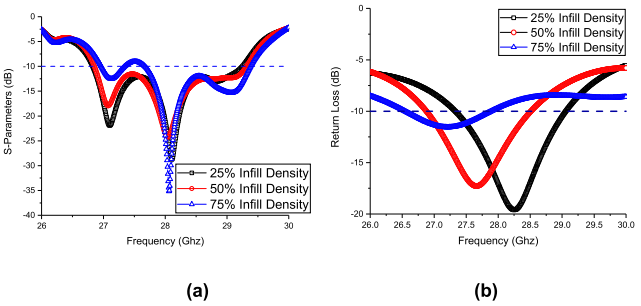

FIGURE 7. Return loss of ILAs for different infill densities of dielectric lens materials (a). SIW (b). MPA.

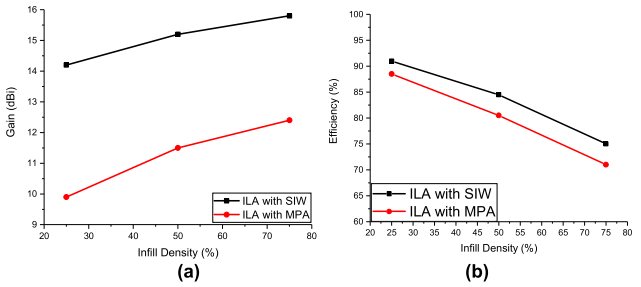

FIGURE 8. (a) Gain and (b) Radiation efficiency for different infill density of dielectric lens material for H/R = 0.3 at 28 GH.

The peak realized gain is approximately constant for all three types of infill patterns, however the rectilinear one exhibits the best results in terms of radiation efficiency and side lobe levels (SLLs), as summarized in Table 2.

The performance of the 3D printed dielectric lenses is affected by the infill density in a similar way to the infill pattern. The density can be varied to tailor the effective relative permittivity and loss tangent of the PLA - air mixture. The impact of infill density on both gain and return loss is shown in Fig. 6(a) and Fig. 7(a) for the SIW slot antenna and Fig. 6(b) & Fig. 7(b) for the MPA array. It is also summarized in Fig. 8, for a fixed ratio of lens height to lens radius. It is evident that the gain is directly proportional to the infill density, whereas radiation efficiency is inversely proportional as shown in Fig. 8(a) and Fig. 8(b), respectively.

After analyzing the results of the parametric study, it is concluded that the gain of ILAs is directly related to the infill density of the lens dielectric material. However, the impact of infill density on gain enhancement needs to be weighed against the impact on other parameters, such as cost, weight and prototyping time. The decision to use 50% for subsequent experimental validation is therefore a trade-off between the gain enhancement on one hand, and the bandwidth, cost, weight, and prototyping time on the other. These factors must be considered in the design of ILAs. All these findings suggest that in-depth studies on infill patterns and infill density are necessary for design and development of dielectric lens antennas using 3D printing technology.

IV. DESIGN OF SOURCE ANTENNAS

Two different antenna arrays were selected to be used as source antennas for the proposed ILAs, to demonstrate the applicability of the design and fabrication process to different scenarios. Both antennas were fabricated in-house at the University of Leeds, using modern PCB fabrication techniques. The substrate used in both cases was the low-loss RT/Duroid^{TM}5880 with relative permittivity $\varepsilon_r = 2.2$ and thickness of 0.787 mm.

A. SIW SLOT ANTENNA

The SIW slot antenna array consists of three SIW cavities, designed according to [22] to support the TE_{102} mode at the center frequency of 28 GHz. The resonant frequency for TE_{m0n} mode of rectangular SIW cavity is given as:

$$f_{mn0} = \frac{c_0}{2\pi\sqrt{\mu_r\varepsilon_r}}\sqrt{\left(\frac{m\pi}{w_{eff}}\right)^2 + \left(\frac{n\pi}{l_{eff}}\right)^2} \quad (1)$$

The width and length of the SIW cavity can be calculated by using equations (2) and (3):

$$w_{eff} = w - \frac{d^2}{0.95p} \quad (2)$$

$$l_{eff} = l - \frac{d^2}{0.95p} \quad (3)$$

The diameter of the via holes and the distance between the two adjacent via holes of SIW should satisfy the conditions [23]:

$$d < \frac{\lambda_g}{5}$$
$$p < 2d \quad (4)$$

where m and n are the mode numbers, w_{eff} and l_{eff} are the effective width and length of the SIW cavity respectively, d is the diameter of via holes and p is the distance between two adjacent via holes, c_0 is the speed of light in vacuum, μ_r and ε_r are the relative permeability and permittivity of the substrate material respectively.

The TE_{102} mode was chosen to support two radiating slots in order to increase the base gain of the SIW slot antenna [11], [24]. The E-field distribution for the TE_{102} cavity mode is shown in Fig. 9(b). In the top metal wall of each cavity, two T-shaped slots are etched over the position of maximum E-field, offset from each other to compensate the 180^0 phase difference between the two adjacent

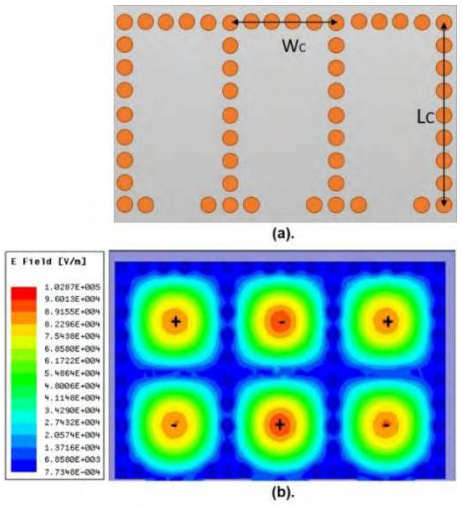

FIGURE 9. (a). SIW cavities and (b). E-field distribution for TE102 mode inside the SIW cavities.

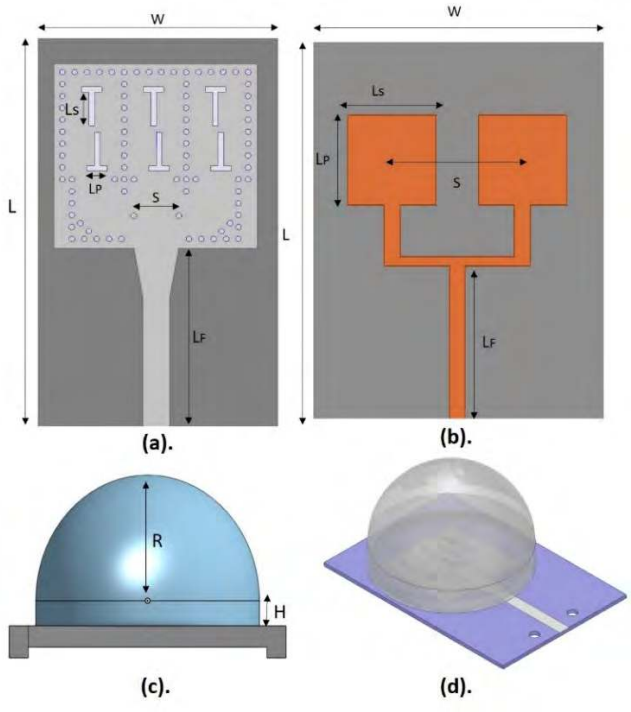

FIGURE 10. Integrated Lens Antennas fed by SIW slot antenna and MPA array (a). SIW slot antenna (b). MPA Array (c). Side symmetric view of dielectric lens (d). Simulation model of ILAs.

E-field peaks. Their linear dimensions and positions were optimized using the commercially available 3D EM simulator Ansys HFSS^{TM}, with the final structure shown in Fig. 10(a). The initial dimensions of the radiating slots were determined as follows [23]:

$$l_s = \frac{\lambda_0}{\sqrt{2(\varepsilon_r + 1)}} \tag{5}$$

$$w_s \leq \frac{l_s}{10} \tag{6}$$

TABLE 3. Final values of design parameters.

Parameter	Value (mm)		Parameter	Values (mm)	
	SIW	MPA		SIW	MPA
L	45	22	L_S	3.6	4
W	31	20	L_P	1.5	3
R	16	8	L_F	20.5	9.5
H	5	2.5	W_C	6	-
S	4	5.5	L_C	18	-

A microstrip line in combination with a SIW power divider is used to feed the SIW cavities and to facilitate connection to test and measurement equipment through a Southwest Microwave 2.4 mm end-launch connector.

B. MICROSTRIP PATCH ANTENNA ARRAY

The second antenna used as a source radiator for the dielectric lens was a simple 2x1 MPA array, again designed for a center frequency of 28 GHz. A microstrip transmission line is used as the feeding network and to connect to the test and measurement equipment, similarly to the SIW slot antenna array. An illustration of the MPA array, together with the physical layout parameters, is show n in Fig. 10(b).

The initial dimensions of the individual patches were determined using standard design method given in [25], before subsequent optimization in Ansys HFSS^{TM}. The center-to-center distance was specified to be $\lambda_0/2$ at 28 GHz, in order to minimize the grating lobes [26].

V. 3D PRINTED DIELECTRIC LENS DESIGN

It has been previously established that dielectric lenses provide an effective way to increase the directivity of a source antenna by reshaping the spherical wave front into a planar one [8], [17]. There are several different types of dielectric lenses [8], and in this paper an extended length hemispherical lens was chosen, due to its straightforward design. An extended hemispherical lens is fully defined by the parameters dome radius R, base diameter $D = 2R$, and base height H [13], which are illustrated in Fig. 10(c).

A parametric analysis of the effect of R and H on antenna directivity is reported in [12], showing that increasing the base height H to radius R ratio increases the directivity of antenna but after a certain value of R/H the directivity starts decreasing. Using these insights, together with the design process described in [18] and [27], the initial values for the lenses were selected and simulation models created, as illustrated in Fig. 10(d). Full-wave EM simulation in the commercially available software package Ansys HFSS^{TM}was then used to optimize the lens parameters for high gain, low return loss, and low side lobe levels (SLLs). The final dimensions are listed in Table 3 for the two ILAs fed by SIW and MPA arrays at 28 GHz.

A. DIELECTRIC LENS FABRICATION

The lenses were fabricated using the commercially available desktop 3D printer (CEL Robox RBX02-DM) using the fused deposition modeling (FDM) technique with a vertical layer

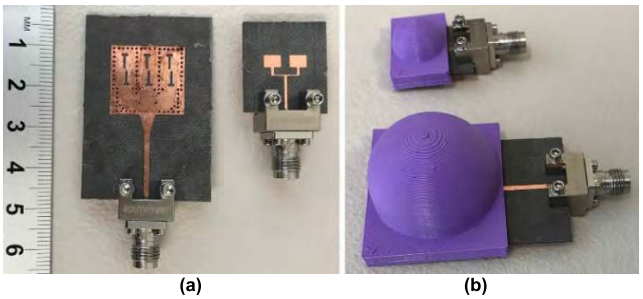

FIGURE 11. Fabricated prototypes of ILAs (a). Source antennas (b). 3D printed dielectric lens on top of source antennas.

resolution of 0.1 mm. The material used was PLA (Polylactic Acid). The reason for choosing PLA is that it is made up of organic materials, so it is safer, easier and more convenient to use for 3D printing as compared to ABS (acrylonitrile butadiene styrene). PLA also has a slightly lower relative permittivity when compared to ABS, which is seen as an advantage, since using a high ε_r material for a dielectric lens has the drawback of excessive internal wave reflections [13]. The lenses were designed, simulated and fabricated using a 50% infill, i.e. only 50% of the internal volume of the lenses is made up of PLA. The infill pattern used was rectilinear one, which gives the best results as compared to triangle and honeycomb infill pattern as discussed in Section III. The geometry of the lens designed in HFSS was exported as a Stereolithographic (STL) format and then imported into 3D-printing slicing and G-code generating software for manual adjustment of the infill density to tailor the permittivity and loss tangent accordingly.

B. LENS ANTENNA INTEGRATION

The integration of 3D printed dielectric lenses on top of source antennas is also a crucial task as well after fabrication of source antennas and dielectric lens antenna individually. A parametric analysis has already been done to optimize the exact position of dielectric lens on top of source antennas. For this purpose, a sliding channel was designed at the base of lenses to easily and accurately integrate and align the source antennas with the 3D printed dielectric lenses as shown in Fig 10(c). The advantage of using a sliding channel was not only the good alignment between the lens and source antenna, but also the avoidance of any adhesive material used to combine the dielectric lens and source antenna that might affect the gain enhancement and radiation patterns of ILAs.

VI. EXPERIMENTAL RESULTS

Several samples of each source antenna, i.e. SIW slot array and 2x1 MPA array, were fabricated and tested, with typical best results presented and discussed here. Photographs of these source antennas, both individually and after integration with the dielectric lenses are shown in Fig. 11(a) and 11(b).

The return loss and the E-plane and H-plane radiation patterns for both antennas, with and without lenses, were measured using the high-frequency measurement facilities at

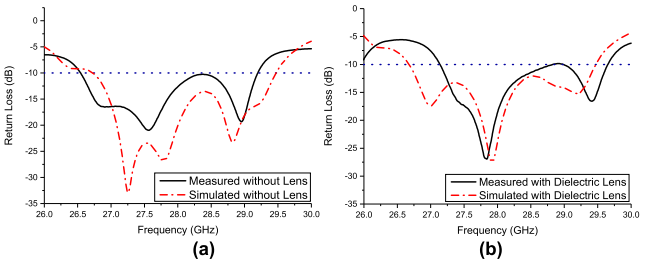

FIGURE 12. S-parameters of SIW slot antenna (a). Without dielectric lens (b). With dielectric lens.

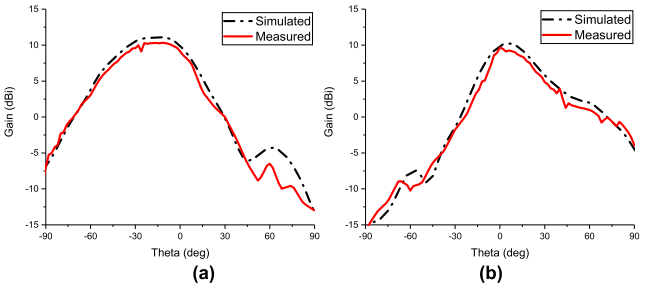

FIGURE 13. Radiation pattern of SIW slot antenna without dielectric lens at 28 GHz (a). E-plane (b). H-plane.

the University of Leeds. A Keysight N5247 PNA-X was used for the S_{11} measurement, with a 1-port mechanical Short, Open, Load (SOL) calibration to bring the reference plane up to the coaxial connector. A Keysight E8361C PNA was used to measure the radiation patterns in a far-field anechoic chamber, using a 20 dBi WR-28 standard gain pyramidal horn antenna as a transmit antenna. The gain at boresight of the proposed antenna was determined using the gain transfer method [28], with two 20 dBi WR-28 reference pyramidal horns used to establish a baseline. These measurements were then compared to the simulation results obtained from Ansys HFSS^{TM}, using the Finite Element Method.

One such comparison for the SIW slot array antenna is presented in Figs. 12-14. A good overall agreement between predicted and measured performance in terms of return loss and radiation pattern is observed in either case, i.e. with and without the dielectric lens mounted on top of the source antenna. The antenna exhibits a wide bandwidth of 2.8 GHz at -10 dB return loss level, from 26.6 GHz to 29.4 GHz, covering most 5G candidate frequency bands. The benefit of the dielectric lens is clearly evidenced by comparing Fig. 13 and Fig. 14. The full-width at half-maximum (FWHM) decreases from 115^0 and 132^0 for the E and H planes, respectively, to 58^0 and 75^0. At the same time, the gain at the centre frequency of 28 GHz is increased from 9.8 dBi to 15.6 dBi.

A similar comparison is shown in Figs. 15-17 for the 2x1 MPA array. Likewise, this antenna design exhibits a wide bandwidth at -10 dB return loss level, spanning the 28 GHz 5G frequency band. However, the gain enhancement in this case is lower, from 8.9 dBi to 12.4 dBi. The increase in directivity is again demonstrated by the reduction in the FWHM at 28 GHz, from $129^0/145^0$ to $90^0/122^0$ for the E/H plane,

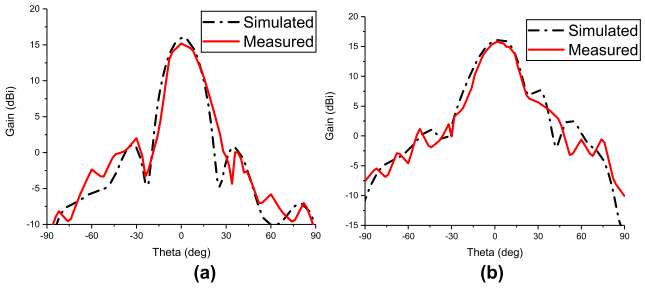

FIGURE 14. Radiation pattern of SIW slot antenna with dielectric lens at 28 GHz (a). E-plane (b). H-plane.

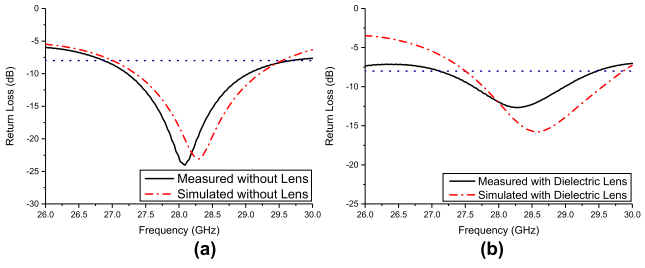

FIGURE 15. S-parameters of MPA array (a). Without dielectric lens (b). With dielectric lens.

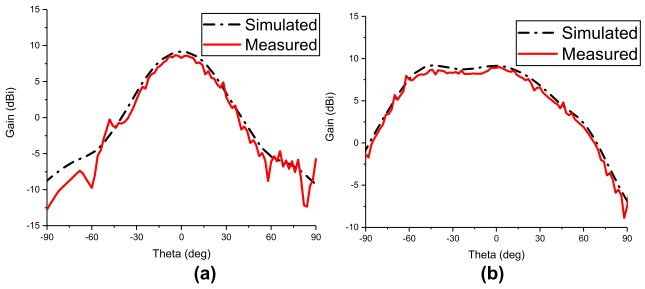

FIGURE 16. Radiation pattern of MPA array without dielectric lens at 28 GHz (a). E-plane (b). H-plane.

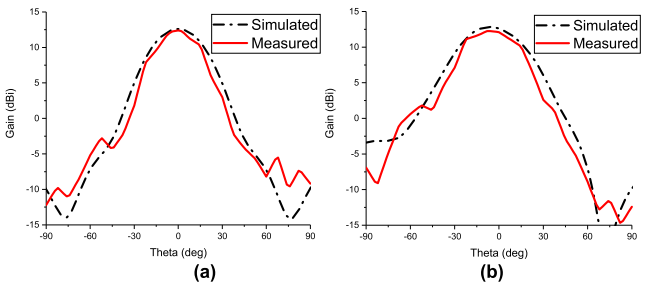

FIGURE 17. Radiation pattern of MPA array with dielectric lens at 28 GHz (a). E-plane (b). H-plane.

respectively. Finally, Fig. 18 demonstrates that the achieved broadband gain is relatively flat over the frequency band of interest, 15.5 $\pm$ 0.5 dBi for the SIW ILA and 12 $\pm$ 0.5 dBi for the MPA ILA.

A summary of the obtained results for the antennas designed and developed in this paper is given in Table 4. At the same time, a comparison on several key metrics with previously published results for dielectric lens antennas at

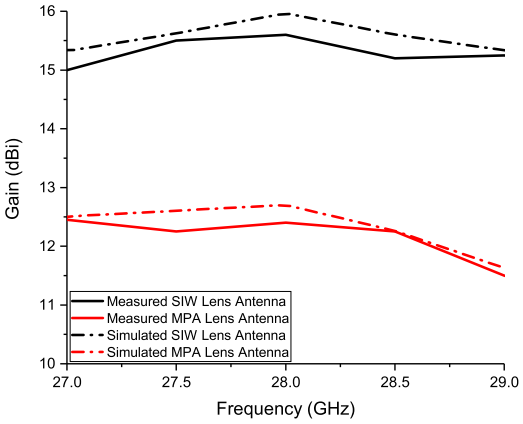

FIGURE 18. Measured gain vs frequency of MPA and SIW with dielectric lens antennas for H/R = 0.3.

TABLE 4. ILAs performance comparison at 28 GHz.

Metric	SIW Slot Antenna	MPA Array
Bandwidth (GHz) with lens	26.6-29.4	27.6-29
Bandwidth (GHz) without lens	26.5-29.5	27.3-29.2
Gain (dBi) with lens	15.6	12.1
Gain (dBi) without lens	9.8	8.9
Side lobe level (dBi)	-20.5	-24
FWHM without lens E/H plane (0)	115/132	129/145
FWHM with lens E/H plane (0)	58/75	90/122
Efficiency (%)	84.5	81.25
Footprint (mm2)	31x45	20x22

similar frequency ranges is presented in Table 5, showing that our dielectric lenses compare favorably in terms of gain, side lobe levels, weight and cost with those produced using more expensive fabrication methods and high-cost and dense dielectric materials.

VII. DISCUSSION AND APPLICATIONS

The reason for using two types of source antennas is to investigate and compare the performance of the proposed low infill 3D printed dielectric lenses for two different scenarios in terms of bandwidth, gain and efficiency. Antennas most commonly used as source antennas under dielectric lenses are the MPAs and SIW slot antennas, due to the ease of their fabrication, straightforward integration with other circuits, low mass and low profile. Dielectric lenses with SIW slot antennas have high bandwidth, gain and efficiency as compared to dielectric lens with MPA. SIW slot antenna have better impedance matching with dielectric lens when we compare the reflection coefficient of SIW slot antenna and MPA after integration with 3D printed dielectric lens in Fig. 12(b) and Fig. 15(b) respectively. In other words, SIW source antennas have more directional radiation pattern and achieve more gain enhancement after integration with dielectric lens as compared to MPAs. Therefore, ILAs with SIW are a promising candidate for 5G mobile communications. On the other hand, dielectric lenses with MPAs are more suitable for phased array and beam steering applications due to their straightforward integration with phase shifters, unlike SIW.

TABLE 5. Comparison of the proposed ILAs with other ILAs reported in open literature.

	[13]	[12]	[15]	[30]	[20]	[31]	[32]	[18]	[6]	Proposed	Proposed
Source Antenna	Waveguide WR-15	Waveguide WR-3	Waveguide WR-15	SIW	MPA	Dipole Array	Helical Antenna	Microstrip aperture coupling	SIW	SIW	MPA
Lens Size (mm)	20	20	10.33	7	15	23	70	44	7	30	16
Frequency Band (GHz)	51-67	230-310	60	18-32	50 – 67	14-20	8.8	28	19.5-32	26.5 – 29.5	27.5 – 29
Gain(dBi)	21.4	30	15	6.2-7.6	13.1	11.2	12.9	11	8	15.5	12.1
SLLs(dB)	-12	-10	-10	-	-23	-11	-16	-15	-16	-20.5	-24
Fabrication Method	SLA 3D Printer	N/A	Poly-jet 3D Printing	N/A	HDI Organic	Industrial Multi-Jet Printing	Industrial Poly-jet printing	CNC	Industrial 3D printing	FDM Desktop 3D Printer	FDM Desktop 3D Printer
Lens Material	Polymer $\varepsilon_r = 2.9$	Rexolite $\varepsilon_r = 3.2$	RGD240 material	Polymer $\varepsilon_r = 3.5$	ABS	Plastic resin	Polymer $\varepsilon_r = 2.6$	Rexolite	PTFE	50% PLA/50% air	50% PLA/50% air
Cost	High	High	High	High	High	Low	High	High	High	Very Low	Very Low

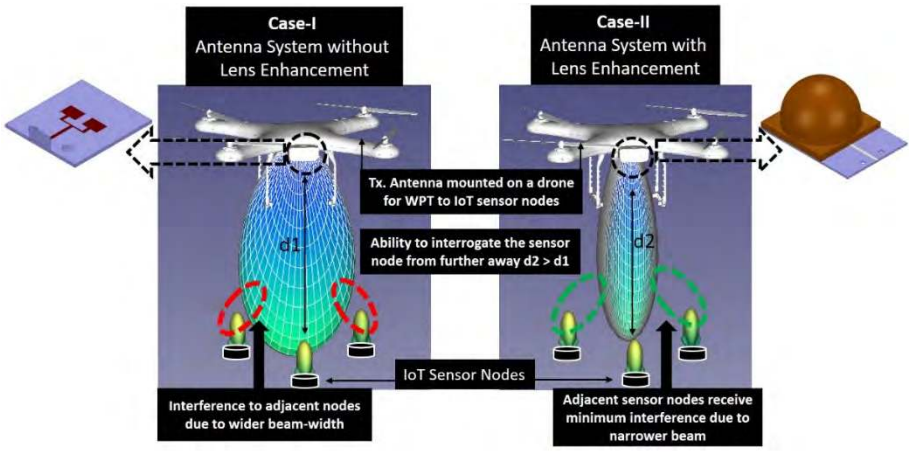

FIGURE 19. Application in Sensor Interrogation using Unmanned Aerial Vehicles.

In our proposed research work we have used low cost 3D printing technology to fabricate low infill dielectric lenses which are efficient, light weight and straightforward to prototype and integrate with source antennas. The ILAs presented in this paper exhibit highly directional radiation patterns with correspondingly high gain, as well as low side lobe levels. Such lens antennas have already been successfully used in several industrial applications for gain enhancement and improving the directionality of the radiation pattern of a source antenna. One such application has been demonstrated in [29], where a hemispherical dielectric lens was integrated on top of a 122 GHz radar front end. The inclusion of this lens has led to a reported improvement in the directionality of the main beam from ±30° FWHM to ±4° FWHM, with a corresponding increase in detection range from 10 m to 100 m.

SIW-fed dielectric lens antennas for satellite communication systems at K/Ka band were presented in [6] and [30]. The basic purpose of using the dielectric lens is to improve the radiation properties source antenna. A wideband circularly-polarized lens antenna is proposed for the 77 GHz automobile radar system [16]. In this case, a hyperbolic lens is fed by a rectangular horn antenna to increase the directivity and decrease the side lobe levels of source antenna for more accurate detection of the target by the radar system.

Finally, lens antennas can have potential applications in unmanned aerial vehicles (UAVs) for high-speed, point-to-point communication with sensor nodes. Using ILAs in this scenario offers several advantages and benefits. One of them is retaining a small footprint while providing a 6 dB gain enhancement. An equivalent increase obtained using a larger array would require a quadrupling of the number of array elements and corresponding occupied area, which may not always be practical. The gain enhancement also provides flexibility from the point of view of the communication link budget. Either the transmitter power can be reduced, which will translate directly to decreased battery usage, or the distance between the UAV and the sensor node can be doubled.

UAVs are known to lose aerodynamic stability and expend more energy when hovering at low altitudes due to the ground effect, therefore this increased distance will improve their flight time as well. In addition to this, the narrower antenna beam would allow the UAV to establish a link with a single node, without causing interference to adjacent ones. These concepts are illustrated in Fig. 19 and will be a subject of a future study by the authors for smart city infrastructure monitoring.

VIII. CONCLUSION

In this paper we have presented a simple, low-cost method of design and fabrication for dielectric lens antennas for wireless communication at millimeter-wave frequencies. The impact of the infill pattern of the 3D-printed dielectric lens on the performance of ILAs and dielectric characterization of 3D-printed PLA samples with varying infill densities have been presented for the frequency range 26-32 GHz. Results for two different types of antennas, usable in different scenarios, are analyzed, and compared. The use of commercially available 3D printing technology with low infill density for the rapid prototyping of highly-efficient dielectric lens antennas is demonstrated. Excellent agreement between simulation and measurement results has been demonstrated.

ACKNOWLEDGMENT

The authors are thankful to the Engineering and Physical Sciences Research Council, UK for the financial support through Grant EP/N010523/1 and the technical staff at the University of Leeds Electronics Workshop for fabricating the antennas presented in this paper.

REFERENCES

[1] J. G. Andrews, S. Buzzi, W. Choi, S. V. Hanly, A. Lozano, A. C. K. Soong, and J. C. Zhang, "What will 5G be?" *IEEE J. Sel. Areas Commun.*, vol. 32, no. 6, pp. 1065–1082, Jun. 2014.

[2] T. S. Rappaport, S. Sun, R. Mayzus, H. Zhao, Y. Azar, K. Wang, G. N. Wong, J. K. Schulz, M. Samimi, and F. Gutierrez, "Millimeter wave mobile communications for 5G cellular: It will work!" *IEEE Access*, vol. 1, pp. 335–349, 2013.

[3] D. Muirhead, M. A. Imran, and K. Arshad, "A survey of the challenges, opportunities and use of multiple antennas in current and future 5G small cell base stations," *IEEE Access*, vol. 4, pp. 2952–2964, 2016.

[4] J. Zhang, X. Ge, Q. Li, M. Guizani, and Y. Zhang, "5G millimeter-wave antenna array: Design and challenges," *IEEE Wireless Commun.*, vol. 24, no. 2, pp. 106–112, Apr. 2017.

[5] R. Bayderkhani, K. Forooraghi, E. Arnieri, B. Abbasi-Arand, and B. S. Virdee, "Analysis of an integrated lens antenna fed by SIW slot array using a hybrid MoM-PO method," *Int. J. Microw. Wireless Technol.*, vol. 9, no. 2, pp. 463–468, 2017.

[6] T. Jaschke, B. Rohrdantz, H. K. Mitto, and A. F. Jacob, "Ultrawideband SIW-fed lens antenna," *IEEE Antennas Wireless Propag. Lett.*, vol. 16, pp. 2010–2013, 2017.

[7] V. M. Pepino, A. F. da Mota, A. Martins, and B.-H. V. Borges, "3-D-printed dielectric metasurfaces for antenna gain improvement in the Ka-band," *IEEE Antennas Wireless Propag. Lett.*, vol. 17, no. 11, pp. 2133–2136, Nov. 2018.

[8] R. Sauleau, C. A. Fernandes, and J. R. Costa, "Review of lens antenna design and technologies for mm-wave shaped-beam applications," in *Proc. 11th Int. Symp. Antenna Technol. Appl. Electromagn. (ANTEM)*, 2005, pp. 1–5.

[9] M. Asaadi and A. Sebak, "High gain low profile slotted SIW cavity antenna for 5G applications," in *Proc. IEEE Int. Symp. Antennas Propag. (APSURSI)*, Jun. 2016, pp. 1227–1228.

[10] T. Mikulasek and J. Lacik, "Two feeding methods based on substrate integrated waveguide for microstrip patch antennas," *IET Microw., Antennas Propag.*, vol. 9, no. 5, pp. 423–430, Apr. 2015.

[11] Q.-L. Yang, Y.-L. Ban, K. Kang, and G. Wu, "SIW multibeam array for 5G mobile devices," *IEEE Access*, vol. 4, pp. 2788–2796, 2016.

[12] K. Konstantinidis, A. P. Feresidis, C. C. Constantinou, E. Hoare, M. Gashinova, M. J. Lancaster, and P. Gardner, "Low-THz dielectric lens antenna with integrated waveguide feed," *IEEE Trans. THz Sci. Technol.*, vol. 7, no. 5, pp. 572–581, Sep. 2017.

[13] K. X. Wang and H. Wong, "Design of a wideband circularly polarized millimeter-wave antenna with an extended hemispherical lens," *IEEE Trans. Antennas Propag.*, vol. 66, no. 8, pp. 4303–4308, Aug. 2018.

[14] N. Chudpooti, N. Duangrit, P. Akkaraekthalin, I. D. Robertson, and N. Somjit, "220-320 GHz hemispherical lens antennas using digital light processed photopolymers," *IEEE Access*, vol. 7, pp. 12283–12290, 2019.

[15] K. X. Wang and H. Wong, "A wideband millimeter-wave circularly polarized antenna with 3-D printed polarizer," *IEEE Trans. Antennas Propag.*, vol. 65, no. 3, pp. 1038–1046, Mar. 2017.

[16] C. Ding and K.-M. Luk, "A wideband high-gain circularly-polarized antenna using artificial anisotropic polarizer," *IEEE Trans. Antennas Propag.*, to be published.

[17] A. Artemenko, A. Mozharovskiy, A. Maltsev, R. Maslennikov, A. Sevastyanov, and V. Ssorin, "2D electronically beam steerable integrated lens antennas for mmwave applications," in *Proc. 42nd Eur. Microw. Conf.*, Oct. 2012, pp. 213–216.

[18] N. T. Nguyen, A. Rolland, A. V. Boriskin, G. Valerio, L. L. Coq, and R. Sauleau, "Size and weight reduction of integrated lens antennas using a cylindrical air cavity," *IEEE Trans. Antennas Propag.*, vol. 60, no. 12, pp. 5993–5998, Dec. 2012.

[19] A. Artemenko, A. Maltsev, A. Mozharovskiy, A. Sevastyanov, V. Ssorin, and R. Maslennikov, "Millimeter-wave electronically steerable integrated lens antennas for WLAN/WPAN applications," *IEEE Trans. Antennas Propag.*, vol. 61, no. 4, pp. 1665–1671, Apr. 2013.

[20] A. Bisognin, D. Titz, F. Ferrero, R. Pilard, C. A. Fernandes, J. R. Costa, C. Corre, P. Calascibetta, J. M. Rivière, A. Poulain, and C. Badard, "3D printed plastic 60 GHz lens: Enabling innovative millimeter wave antenna solution and system," in *IEEE MTT-S Int. Microw. Symp. Dig.*, Jun. 2014, pp. 1–4.

[21] R. Gonalves, P. Pinho, and N. B. Carvalho, "3D printed lens antenna for wireless power transfer at Ku-band," in *Proc. 11th Eur. Conf. Antennas Propag. (EUCAP)*, Mar. 2017, pp. 773–775.

[22] R. Elliott, "An improved design procedure for small arrays of shunt slots," *IEEE Trans. Antennas Propag.*, vol. 31, no. 1, pp. 48–53, Jan. 1983.

[23] S. Moitra, A. K. Mukhopadhyay, and A. K. Bhattacharjee, "Ku-band substrate integrated waveguide (SIW) slot array antenna for next generation networks," *Global J. Comput. Sci. Technol.*, to be published.

[24] J. F. Xu, W. Hong, P. Chen, and K. Wu, "Design and implementation of low sidelobe substrate integrated waveguide longitudinal slot array antennas," *IET Microw., Antennas Propag.*, vol. 3, no. 5, pp. 790–797, Jul. 2009.

[25] J. L. Volakis, R. C. Johnson, and H. Jasik, *Antenna Engineering Handbook*, 4th ed. New York, NY, USA: McGraw-Hill, 2007, p. 1818.

[26] R. J. Mailloux, *Phased Array Antenna Handbook*. Norwood, MA, USA: Artech House, 2005, p. 496.

[27] H. P. Yin and W. B. Dou, "Analysis of an extended hemi-spherical lens antenna at millimeter wavelengths," *J. Electromagn. Waves Appl.*, vol. 16, no. 9, pp. 1209–1222, 2002.

[28] *IEEE Standard Test Procedures for Antennas*, ANSI/IEEE Standard 149–1979, 1979.

[29] Silicon Radar. (2019). *EvalKits for Radar Front Ends*. Accessed: Jul. 5, 2019. [Online]. Available: https://siliconradar.com/evalkits/

[30] T. Jaschke, H. K. Mitto, and A. F. Jacob, "K/Ka-band dual-polarized SIW-fed lens antennas for Rx/Tx integration," *Int. J. Microw. Wireless Technol.*, vol. 10, nos. 5–6, pp. 627–634, 2018.

[31] Y.-X. Zhang, Y.-C. Jiao, and S.-B. Liu, "3-D-printed comb mushroom-like dielectric lens for stable gain enhancement of printed log-periodic dipole array," *IEEE Antennas Wireless Propag. Lett.*, vol. 17, no. 11, pp. 2099–2103, Jun. 2018.

[32] M. F. Farooqui and A. Shamim, "A 3D printed helical antenna with integrated lens," in *Proc. IEEE Int. Symp. Antennas Propag. USNC/URSI Nat. Radio Sci. Meeting*, Jul. 2015, pp. 324–325.

BILAL TARIQ MALIK was born in Pakistan, Islamabad, in 1988. He received the B.Sc. and M.Sc. degrees from the Electrical Engineering Department, COMSATS University Islamabad, Pakistan, in 2011 and 2014, respectively. He received the Institute Silver Medal & Campus Bronze Medal for the B.Sc. degree from COMSATS University Islamabad, Pakistan. He is currently pursuing the Ph.D. degree in electronics and electrical engineering from the University of Leeds, U.K. He is fully funded by Leeds Anniversary Research Scholarship (LARS), University of Leeds. He was a Research Associate with the Electrical Engineering Department, COMSATS University Islamabad, where he was involved in various research projects and teaching. His current research interests include millimeter-wave antenna arrays, rectennas for far-field wireless power transfer, and 5G communications.

VIKTOR DOYCHINOV received the B.Eng. degree in telecommunications from the Technical University of Sofia, Bulgaria, in 2009, the M.Sc. degree in spacecraft technology and satellite communications from University College London, U.K., in 2011, and the Ph.D. degree in electronic and electrical engineering from the University of Leeds, U.K., in 2016. Since 2016, he has been a Research Fellow with the School of Electronic and Electrical Engineering, University of Leeds, where he was involved in high-frequency engineering. His current research interests include microwave and millimeter-wave circuits and antennas, biomedical applications of wireless technology, and wireless communications in complex environments.

SYED ALI RAZA ZAIDI received the Ph.D. degree from the School of Electronic and Electrical Engineering, University of Leeds, Leeds. From 2011 to 2013, he was associated with the International University of Rabat as a Lecturer. From 2013 to 2015, he was associated with the SPCOM Research Group, U.S. Army Research Laboratory, and funded project in the area of network science. In 2013, he was also a Visiting Research Scientist with the Qatar Innovations and Mobility Center, where he was involved in QNRF funded project QSON. He is currently a University Academic Fellow (Assistant Professor) in wireless communication and sensing systems with the University of Leeds. He has published more than 90 papers in leading IEEE conferences and journals. He is also an Active Member of the EPSRC Peer Review College. During his Ph.D. degree, he received the G. W. Carter Prize and the F. W. Carter Prize for best thesis and best research paper, respectively. He is a EURASIP Local Liaison for U.K., and also a General Secretary of the IEEE Technical Subcommittee on Backhaul and Fronthaul Networks. From 2014 to 2015, he served as an Editor for the IEEE COMMUNICATION LETTERS. He was also a Lead Guest Editor of *IET Signal Processing Journal*'s Special Issue on Signal Processing for Large-Scale 5G Wireless Networks. He is currently an Associate Technical Editor of the *IEEE Communication Magazine*.

IAN D. ROBERTSON received the B.Sc. (Eng.) and Ph.D. degrees from King's College London, London, U.K., in 1984 and 1990, respectively.

From 1984 to 1986, he was with the GaAs MMIC Research Group, Plessey Research, and Caswell, U.K. After that, he returned to King's College, initially as a Research Assistant, working on the T-SAT Project, subsequently as a Lecturer, leading the MMIC Research Team, and becoming a Reader, in 1994. In 1998, he became a Professor of microwave subsystems engineering with the University of Surrey, where he established the Microwave Systems Research Group, and was a Founding Member of the Advanced Technology Institute. In 2004, he was appointed to the Centenary Chair in microwave and millimetre-wave circuits with the University of Leeds. He was the Director of learning and teaching from 2006 to 2011, and also the Head of the School from 2011 to 2016.

Dr. Robertson was the General Technical Programme Committee Chair for the European Microwave Week, in 2011 and 2016.

NUTAPONG SOMJIT received the Dipl.Ing. (M.Sc.) degree from the Dresden University of Technology, in 2005, and the Ph.D. degree from the KTH Royal Institute of Technology, in 2012. Then, he returned to the Dresden University of Technology to lead a research team in micro-sensors and MEMS ICs for the Chair for Circuit Design and Network Theory. In 2013, he was appointed as a Lecturer (Assistant Professor) with the School of Electronic and Electrical Engineering, University of Leeds. His current research interests include integrated smart high-frequency components, heterogeneous integration, and low-cost microfabrication processes.

He was appointed as a member of the Engineering, Physical and Space Science Research Panel of the British Council, in 2014. Since 2013, he has been a member of the International Editorial Board of the *International Journal of Applied Science and Technology*. He was a recipient of the Best Paper Award (EuMIC Prize) at the European Microwave Week, in 2009. He received a Graduate Fellowship from the IEEE Microwave Theory and Techniques Society (MTT-S), in 2010 and 2011, and the IEEE Doctoral Research Award from the IEEE Antennas and Propagation Society, in 2012. In 2016, he was the Chair of the Student Design Competition for the European Microwave Week. In 2018, he was appointed as an Associate Editor of *Electronics Letters*.